Anonymous Referee #2

This paper introduces a novel methodology for identifying coastal morphological changes using Longitudinal Wave Power (LWP) as a proxy, moving beyond traditional significant wave height (Hs) approaches. The integration of LWP with optimized POT parameters represents a significant advancement over conventional Hs-based approaches. The paper is well-structured with clear methodology sections, comprehensive figures, and detailed supplementary materials. However, the paper still presents some weakness that need to be resolved. Please find below my detailed comments:

The authors sincerely thank Reviewer 2 for their careful reading and insightful comments on our manuscript. Following their guidance, we have significantly revised the manuscript and added a new section regarding its application to real-world scenarios. To address the concerns about the absence of field data, we have now implemented the methodology using real-world models of two different study areas along the South Atlantic coast of the Iberian Peninsula. These applications were carried out using previously calibrated and validated numerical models, whose calibration and validation were performed against real measured bathymetric data. This provides a meaningful empirical grounding for the methodology beyond the idealized framework, while also introducing real-world forcings including observed wave conditions, complete tidal regimes, and variable river discharges, and also different sediment grain sizes.

1. **The most significant limitation is the experiments and findings rely on idealized numerical simulations without comparison to observed coastal morphological data. While the authors acknowledge the difficulty in obtaining synchronized hourly resolution data, the lack of any field validation severely limits confidence in the methodology's real-world applicability.**

Following the reviewers' suggestions, a new section has been incorporated into the manuscript to present the application of the methodology to two real-world study areas. These applications were carried out using previously calibrated and validated numerical models, whose calibration and validation were performed against real measured bathymetric data. This provides a meaningful empirical grounding for the methodology beyond the idealized framework, while also introducing real-world forcings including observed wave conditions, complete tidal regimes, and variable river discharges, and also different sediment grain sizes. As shown in the revised manuscript, the new Section 5, "Application to real-world study areas", reads as follows:

"*The methodology was applied to two different real-world study areas: the Punta Umbría Inlet, following Zarzuelo et al. (2019) and the Guadiana estuary, following López-Ruiz et al. (2020). For both study cases, models were implemented in Delft3D and have been calibrated and validated against field-measured bathymetric surveys, providing continuous morphological simulations over real observed periods. For the Punta Umbría Inlet, the model spans from July 2014 to October 2015, with model data obtained at 3-hour intervals. For the Guadiana estuary, two separate simulations with hourly data were utilized: (1) from July 2016 to June 2017, and (2) from June 2017 to December 2018. This section presents the match results for each simulation using the two primary POT combinations: T-POT and Combination 11.*

5.1. Punta Umbría Inlet

The Punta Umbría Inlet (hereinafter PUI) consists of a NW-SE trending channel, 8 km in length and 0.5 km in width, with a maximum depth of -12 m MSL. Characterized as an ebb-tidal system, it features minor ebb channels, shoals, and frontal lobes. The model utilizes a spatially distributed D_{50} sediment grain size, ranging from 0.5 to 4 mm. This is defined via a grid-based input file to reflect the natural variability of the seabed. Due to long-standing navigational difficulties associated with shoal development, a jetty was constructed at the inlet, reaching -4 m MSL. The numerical setup and validation procedures follow Zarzuelo et al. (2019) in their entirety. A comprehensive description of the model performance is available in that study.

The control volume used to apply the methodology is located in the channel (Figure S11 from Supplementary Material). The match values obtained for the T-POT are 43.4% and 41.4% for the LWP-ME90 and LWP-ME95, respectively, and 42,7% and 45,1% for the H_s-ME90 and H_s-ME95, respectively. For the optimal combination (Combination 11, POT(95,4,6)), the match results for LWP increase to 47.4% (ME90) and 47.5% (ME95), while the H_s matches remain identical to those of the T-POT. This suggests that the optimal POT combination improves upon the T-POT for LWP while maintaining the same accuracy for H_s.

5.2. Guadiana estuary

The numerical setup for the Guadiana estuary follows the configuration described in López-Ruiz et al. (2020), where a comprehensive description of the model's calibration and performance is available. The study area encompasses the ebb-tidal delta of the Guadiana River, located at the southern border between Spain and Portugal. The region is characterized by a semi-diurnal mesotidal regime, with a mean tidal range of 2 m. Similar to the PUI, the river mouth is stabilized by a jetty system, and the main channel undergoes periodic dredging to maintain navigability. Sediment distribution in the area exhibits the high variability typical of deltaic environments, with grain sizes ranging from fine to coarse sands. The model utilizes a spatially distributed D_{50} sediment grain size, ranging from 1 to 10 mm. This is defined via a grid-based input file to reflect the natural variability of the seabed.

Two simulations covering different periods are available for this study area, hereafter referred to as Guadiana 1617 (from July 2016 to June 2017) and Guadiana 1718 (from June 2017 to December 2018). The control volume used to apply the methodology is located in the ebb delta, within an area comparable to the one analyzed by Garel et al. (2019) to unravel the sediment transport patterns in the delta (Figure S12 from Supplementary Material).

For Guadiana 1617, the match values obtained for the T-POT are 63.5% and 62.9% for the LWP-ME90 and LWP-ME95, respectively, and 64.3% and 63.9% for the H_s-ME90 and H_s-ME95, respectively. For the optimal combination (Combination 11, POT(95,4,6)), the match results for LWP increase to 67.5% (ME90) and 67.9% (ME95), while the H_s matches remain identical to those of the T-POT.

For the Guadiana 1718 period, the T-POT achieved match values of 72.3% and 90.5% for LWP (ME90 and ME95, respectively), and 73.1% and 90.5% for H_s. The optimal POT combination (Combination 11) improved the LWP-ME90 match to 79% and the H_s-ME90 to 74.4%, while maintaining identical results for all ME95 events. Notably, almost all ME95 morphological events occurred during Storm

Emma (February 2018), which heavily impacted the South Atlantic coast of the Iberian Peninsula (Málvarez et al. 2021).”

As demonstrated, the application to real-world scenarios confirms the robustness of the methodology. The optimal POT combination (Combination 11) consistently outperforms the T-POT across the three simulations analyzed regarding LWP matches. The single exception is the Guadiana 1718 case, where the dominance of a single extreme event (Storm Emma) concentrates nearly all ME95 events within a brief period, thereby limiting the discriminatory capacity of the LWP-based proxy under such specific conditions. This behavior is consistent with the role of the LvC index discussed in Section 6.1 of the revised manuscript (and further detailed in our response to Comment 1), reinforcing the complementary nature of LWP and Hs as morphological proxies. Moreover, the Hs related matches for the optimal POT combination are equal to the T-POT matches, with the exception of Guadiana 1718, where the match for Hs-ME90 shows an improvement over the T-POT.

Storm Emma (February 28 – March 5, 2018) was a severe Atlantic event that triggered extreme meteorological and oceanographic conditions across the southwestern Iberian Peninsula. It produced a 22-year record significant wave height of 7.27 m and raised sea levels to 4.12 m through a combination of low atmospheric pressure and spring tides. These forces caused profound morphodynamic changes, including dune erosion of 2.5 m and the modification of seabed elevation at depths as great as -10 m (García-de-Lomas, et al., 2019; Málvarez et al. 2021).

The Figures S11 and S12 from the Supplementary Material correspond to Figure 1 and Figure 2, respectively, from the attached document.

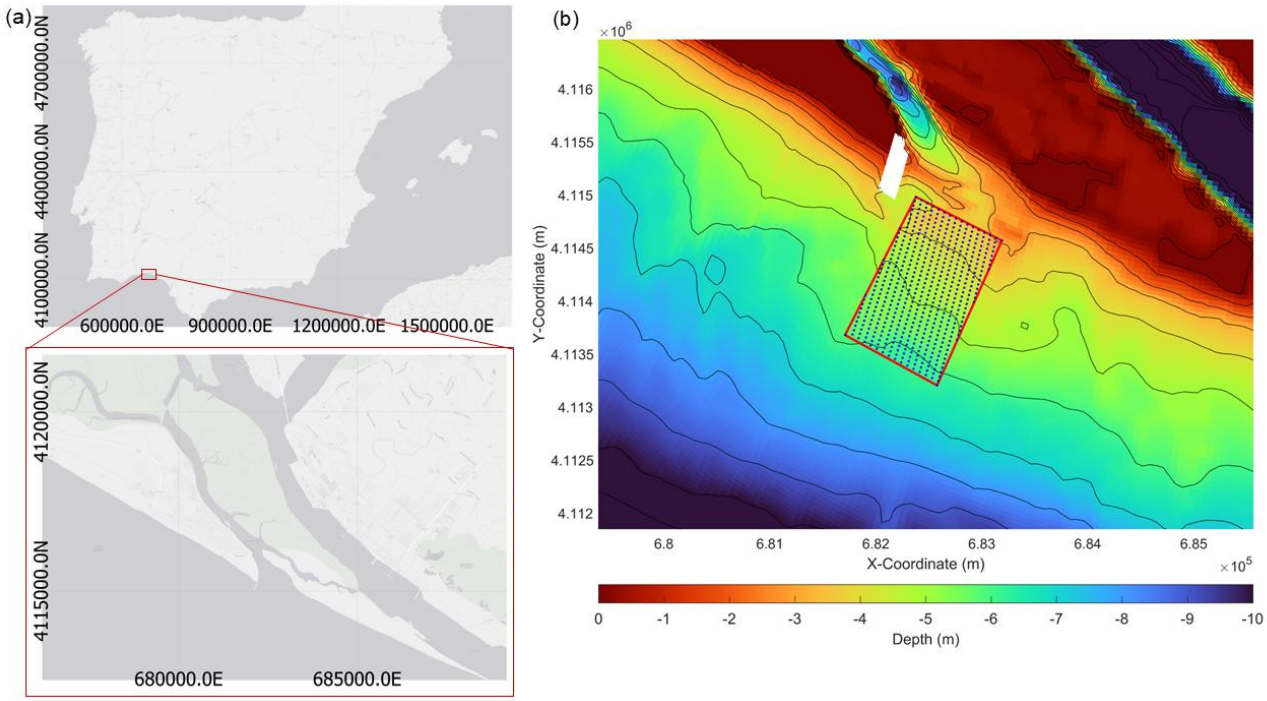

Figure 1. (a) Study area location in the Iberian Peninsula. (b) Control volume for the Punta Umbría Inlet shown on the actual bathymetry of the area. Bathymetric contours are represented every 1m, from 0 to -12 m MSL.

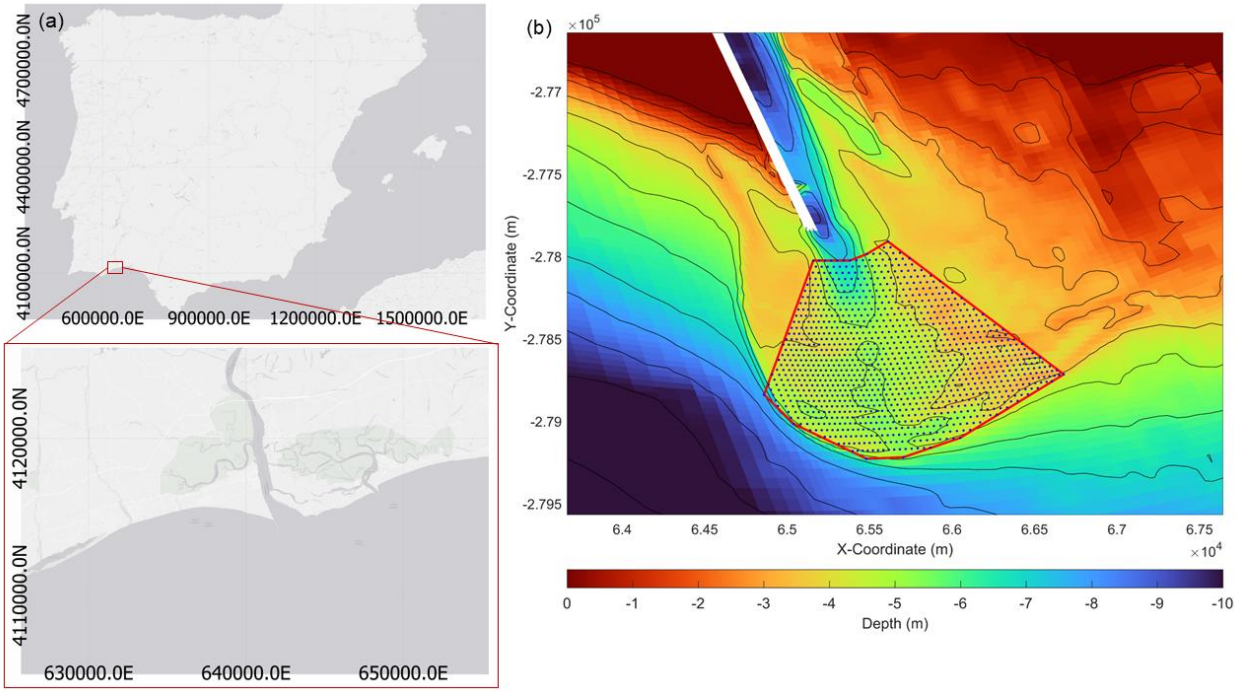

Figure 2. (a) Study area location in the Iberian Peninsula. (b) Control volume for the Guadiana Estuary shown on the actual bathymetry of the area. Bathymetric contours are represented every 1 m, from 0 to -12 m MSL.

1. **The study uses only a single sediment size (D50 = 1 mm), constant river discharge (10 m³/s), and a specific synthetic tidal regime (M2 and S2). These constraints limit application to complicated coastal environments. For example, the commonly used harmonic analysis for ocean tide generally include 8 major components. In addition, some sensitivity analysis for fine sands (D50 = 0.2-0.5 mm) or coarser sediments (D50 = 2-5 mm) may benefit.**

The authors acknowledge the referees' concerns regarding the simplified initial conditions. Regarding sediment grain size, following their guidance two additional simulations were conducted as a sensitivity analysis. Using Experiment 1 (1980–1981) as a baseline, we modified the original D_{50}=1mm in the simulation to D_{50} = 0.5 mm and D_{50} = 2mm.

Table 1. Match percentages obtained for different D_{50} values during the sensitivity analysis of Experiment 1 (1980–1981).

1980-1981		LWP-ME90		Hs-ME90		LWP-ME95		Hs-ME95	
		NCV	SCV	NCV	SCV	NCV	SCV	NCV	SCV
T-POT	**Original (D_{50} = 1mm)**	**49.4**	**55.8**	**34.1**	**32**	**65.5**	**82.5**	**53.4**	**55.6**
	D_{50} = 0.5 mm	38.4	68.8	28.4	45.1	41.2	88.7	39.8	61.8
	D_{50} = 2 mm	53.3	46,47	30.8	22.3	78.2	60.3	54.7	35.8
Optimal POT combination	**Original (D_{50} = 1mm)**	**53.2**	**55,78**	**37.1**	**35.5**	**72.9**	**82.5**	**53.4**	**62.6**
	D_{50} = 0.5 mm	38.4	68.8	31.6	49.5	41.2	88.7	39.8	69.2
	D_{50} = 2 mm	57.4	46.5	33.3	25.7	78.2	60.3	54.7	43.1

The results, presented in Table 1, show that the overall effectiveness of the methodology persists across different grain sizes. Specifically, a clear trend of improvement in the match related to LWP is observed in certain configurations, and the optimal POT combination consistently yields equal or higher match percentages compared to the traditional approach. Even having changes on the values according to the grain size, the overall match values are reasonably similar, with a difference that is lower than 10% for the majority of the tested conditions when referred to the original used value (D50 = 1 mm). However, given the current length of the manuscript and the addition of the new section featuring real-world data, we have decided to omit this specific information to maintain conciseness.

Regarding the tidal regime, the use of only two tidal components (M2 and S2) follows established approaches in the literature for morphodynamic simulations of river mouth systems (e.g., Jiménez-Robles et al., 2016; Ruiz-Reina & López-Ruiz, 2021). The primary objective was to reproduce the dominant tidal forcing in a controlled manner, rather than to replicate the full spectral complexity of a real tidal signal.

Similarly, the use of a constant river discharge in the idealized simulations was a deliberate methodological choice. In this context, the constant discharge allows us to isolate the morphological response driven specifically by wave-induced processes, minimizing the confounding influence of fluvial forcing on the results.

However, we believe that the application of the methodology to real-world scenarios, as discussed in the previous response and in the revised manuscript, addresses these concerns. In those cases, the bathymetries reflect natural sediment variability (including spatially distributed D_{50}), and the forcing inputs are based on empirical data, including complete tidal regimes, variable river discharges, and explicit wind forcing alongside buoy-derived wave data. Furthermore, the concurrent increase in river discharge during storm events is a physically relevant process —particularly in fluvially influenced systems such as the Guadiana estuary and the Punta Umbría Inlet — which is now explicitly accounted for in our real-world validation.

The results demonstrate that the methodology remains robust even when these additional environmental complexities are introduced. Since the effectiveness of the approach is captured in both controlled idealized cases and complex natural environments, we believe the current scope provides a comprehensive validation of its robustness.

To further clarify this point (and the related to the previous comment), we have added a discussion of these considerations in Section 6.3 (formerly Section 5.3) “Limitations and further improvements” , which now reads: *“Although the method was developed following established idealized frameworks (e.g., Jiménez-Robles et al., 2016; Ruiz-Reina & López-Ruiz, 2021), its successful validation in calibrated environments with real-world forcings, which include wind, variable river discharge, and full tidal regimes, addresses the applicability to complex coastal zones and supports the robustness of the methodology under more complex forcing conditions.”*

2. **Another problem is the exclusion of wind effects. The storm impacts on morphological changes are an important part of this paper but the contribution of winds seems totally ignored, which potentially weaken the value of these findings.**

We thank the reviewer for raising this point. Consistent with our previous responses, the exclusion of explicit local wind forcing from the idealized simulations was a deliberate methodological choice, consistent with established idealized morphodynamic modeling frameworks (see previous response) to avoid additional non-linearities, as local wind forcing would complicate the isolation of morphological responses driven purely by wave-induced processes.

This limitation is mitigated in the real-world applications presented in the new Section 5, where both models incorporate explicit wind forcing alongside buoy-derived conditions. Our results demonstrate that the methodology remains effective in both cases, suggesting that the presence of explicit wind forcing does not compromise the application or the reliability of the findings. Moreover, while the idealized model does not explicitly include local wind forcing, the wave conditions are derived from buoy data, which inherently capture the energy transferred by wind.

To further clarify this point (and the related to the previous comment), we have added a discussion of these considerations in Section 6.3 (formerly Section 5.3) "Limitations and further improvements" , which now reads: *"Although the method was developed following established idealized frameworks (e.g., Jiménez-Robles et al., 2016; Ruiz-Reina & López-Ruiz, 2021), its successful validation in calibrated environments with real-world forcings, which include wind, variable river discharge, and full tidal regimes, addresses the applicability to complex coastal zones and supports the robustness of the methodology under more complex forcing conditions."*

3. **I am not sure about the definition of the CI. What is the reason for the 70-30 weighting? Was any optimization performed to determine these weights?**

Regarding the CI index, our objective was to prioritize the average performance of the metrics while still accounting for their variability across different wave climates.

The primary objective of the CI is to identify the POT combination that most effectively captures morphologically significant events across all simulated years. The mean match percentage is the most direct measure of this overall effectiveness and therefore receives the higher weight (70%). The standard deviation, in contrast, quantifies the variability of the match across different wave climates, which is a secondary but relevant consideration: a combination that performs well on average but inconsistently across years is less reliable than one that achieves a similarly high mean with lower variability. A weight of 30% was assigned to reflect this secondary role. Consequently, the dispersion remains a critical factor in identifying climates where the proxy performs more consistently (a behavior related to the LvC index explained in the response to question 6).

Furthermore, the 70-30 weighting is consistent with the trends observed in Figures 6 and 7, which demonstrate that this balance best represents the overall stability of the results across the tested scenarios. Finally, the application of the methodology to the real-world scenarios (new Section 5, question 1) confirms these findings, as the optimized POT combination identified by the CI yielded a higher match and superior performance, further validating it.

4. **I would recommend adding boundary conditions in the Fig. 1 to clearly illustrate their settings.**

The figure has been modified following the reviewer's suggestion. The revised Figure 1 (Figure 3 from the present document) is as follows:

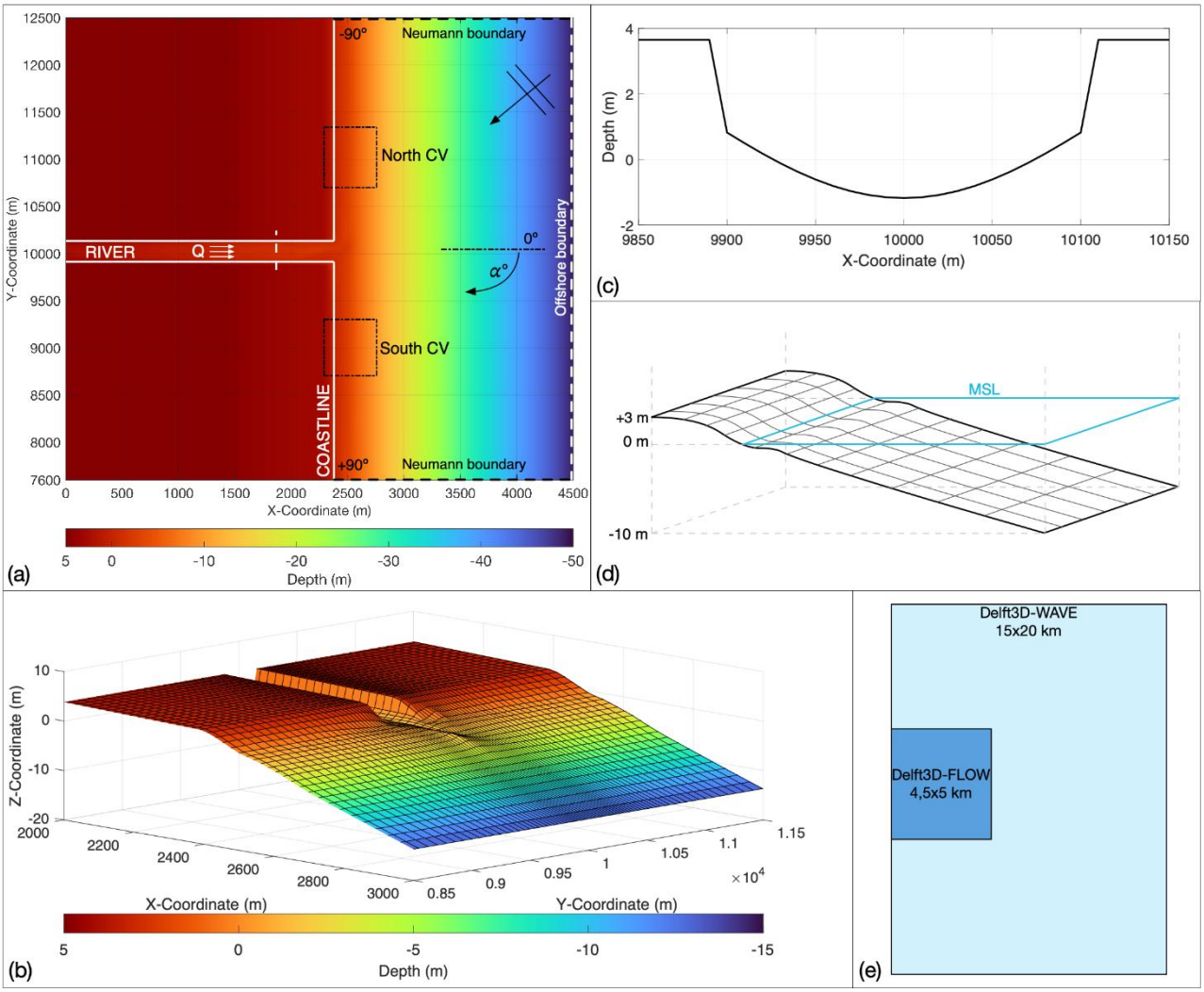

Figure 3 - Physical scenario: (a) and (b) depict the smoothed bathymetry (basic state) used for the simulations; (a) plan view where the dashed black line represents shore-normal incident waves, with positive (negative) values indicating waves coming from the South (North) part of the figure, and the white arrows on the river channel indicates the flow discharge (Q); (b) 3D view; (c) channel cross-section corresponding to the dashed white line position in (a); (d) representation of the surface (with variable grid) and the limits for the volume calculated in each control volume (CV) depicted in (a); and (e) the Delft3D-FLOW domain embedded into a larger Delft3D-WAVE domain; note that the FLOW domain is coupled with the WAVE domain.

5. **Although the mean significant wave heights for the six years are similar, Table 1 shows significant differences in total wave power (e.g., Exp 5 and Exp 6). Are these differences caused by storm frequency or duration? How might these variations in wave climate characteristics affect the applicability of the optimal POT parameters under different climate conditions?**

We acknowledge the reviewer's observation. The climate analysis (Table 1 of the manuscript) indicates that the differences in total wave power between experiments are driven by a combination of storm

frequency and intensity, rather than a single factor or a simple linear relationship with the number of storm days.

Taking Experiments 5 (2010–11) and 6 (2019–20) as an illustrative example, Experiment 5 exhibits significantly higher energy levels (+104 kW/m) and more extreme peaks, with a Hs 99th percentile of 3.76 m compared to 3.33 m in Experiment 6. This higher total wave power is further explained by a greater number of energetic events exceeding the 95th percentile threshold. A detailed breakdown of storm frequency and energy metrics for all experiments is provided in Table 1 of the manuscript.

We have clarified the difference between the inter-annual variability in Section 2.2. "Hydrodynamic Forcings" of the revised manuscript, which now reads as follows: "*While mean Hs values were similar (1.00–1.11 m), the most extreme waves (e.g. Hs 99th) showed greater variability, ranging from 2,89 m to 3,76 m (Table 1). This selection focuses on a single representative site to evaluate the methodology's sensitivity to inter-annual variability in wave energy distribution, rather than climatic shifts across different locations. This approach ensures consistency in regional characteristics while maintaining a manageable computational cost for high-resolution event-based analysis*".

Regarding the applicability of the optimal POT parameters, our results demonstrate that although the match percentages fluctuate depending on the year's energy (e.g., higher H_s match in Exp 5 vs. improved LWP match in Exp 6), the optimal combination (Combination 11) consistently outperforms the standard T-POT across all scenarios. This suggests that the methodology is robust to inter-annual climate variations at the site.

Moreover, to take into account the applicability of the optimal POT parameters under different climate conditions, the Longshore vs. Cross-shore index proposed by López-Dóriga and Ferreira (2017) (LvC index) was implemented. This index relates wave energy conditions to volumetric sediment changes to determine whether a storm event or coastal area is longshore-dominated or cross-shore-dominated. This information was incorporated into the present study in section 6.1 "The role of wave direction" (formerly Section 5.1) of the revised manuscript, reading as follows: "*Furthermore, by applying the LvC (Longshore vs. Cross-shore) index proposed by López-Dóriga and Ferreira (2017), it was found that the NCV exhibits a more cross-shore dominated in experiment 2 (1990-91) with an LvC=0.18, and in experiment 5 (2010-11) with LvC=0.01, both of which correspond to a higher H_s-match. Conversely, the SCV shows systematically higher LvC across most experiment, indicating a greater degree of longshore dominance, which corresponds with a higher LWP-match. The calculated LvC indices for all experiments and control volumes are provided in Table S5 of the Supplementary Material.*".

Table S5 from the Supplementary Material corresponds to Table 2 of the present document.

Table 2. LvC index calculated for each CV and for each experiment.

Year (Experiment)	NCV	SCV
1980-1981 (1)	0.25	0.30
1990-1991 (2)	0.18	0.60
1999-2000 (3)	0.85	0.66
2000-2001 (4)	0.38	0.44
2010-2011 (5)	0.01	0.40
2019-2020 (6)	0.17	0.75

6. **Lines 455-465 & Figures 8-9: The statistical analysis reveals that POT combinations with 48-hour minimum duration show drastically reduced performance. This suggests that morphologically significant events in your study area are characterized by short-lived, high-intensity impulses. How would this finding translate to regions with different storm characteristics, such as tropical cyclone environments where sustained wind conditions may persist for days?**

The authors acknowledge the concern regarding the generalization of the method. However, it should be noted that the methodology and the optimal POT parameters are calibrated for the wave climates observed along the Andalusian coast, which is characterized by an oceanic-influenced Mediterranean climate on its Atlantic side and a typical Mediterranean climate in the Mediterranean side. The Atlantic coast of Andalusia is characterized by a transitional oceanic-Mediterranean climate in which energetic storm events are typically short-lived and associated with high peak wave heights rather than sustained forcing over multiple days. In this context, requiring a minimum storm duration of 48 hours to define a POT event results in the exclusion of numerous short but morphologically significant events, thereby reducing the match between identified climatic events and observed morphological changes.

As stated by Almarshed (2025), POT parameters are context-specific and vary across different geographic regions. Therefore, when applying this method to areas characterized by tropical cyclone environments or sustained storm conditions, a site-specific re-optimization of the POT parameters would be necessary to capture the different temporal and intensity scales of those events.

In tropical cyclone environments, where sustained forcing may persist for several days, longer minimum duration thresholds would likely yield better performance, and a site-specific re-optimization of the POT parameters would be required. However, it is important to distinguish between the site-specificity of the optimal parameters and the generalizability of the methodological framework itself: the LWP-based POT approach proposed in this study is applicable to any coastal environment, provided that the POT parameters are calibrated locally using representative morphological and wave data

Overall, the paper represents good work that merits publication after major revisions.

References cited in the response

Almarshed, B. F.: Optimizing threshold selection for accurate prediction of long-term extreme wave heights, Journal of Engineering Research (Kuwait), 13, 2965–2983, https://doi.org/10.1016/j.jer.2024.12.005, 2025.

García-de-Lomas, J., Payo, A., Cuesta, J. A., and Macías, D.: Morphodynamic study of a 2018 mass-stranding event at Punta Umbria Beach (Spain): Effect of Atlantic Storm Emma on Benthic Marine Organisms, J Mar Sci Eng, 7, https://doi.org/10.3390/jmse7100344, 2019.

Jiménez-Robles, A. M., Ortega-Sánchez, M., and Losada, M. A.: Effects of basin bottom slope on jet hydrodynamics and river mouth bar formation, J Geophys Res Earth Surf, 121, 1110–1133, https://doi.org/10.1002/2016JF003871, 2016.

López-Dóriga, U. and Ferreira, Ó.: Longshore and cross-shore morphological variability of a berm-bar system under low to moderate wave energy, J Coast Res, 33, 1161–1171, https://doi.org/10.2112/JCOASTRES-D-16-00050.1, 2017.

Málvarez, G., Ferreira, O., Navas, F., Cooper, J. A. G., Gracia-Prieto, F. J., and Talavera, L.: Storm impacts on a coupled human-natural coastal system: Resilience of developed coasts, Sci. Total Environ., 768, 144987, https://doi.org/10.1016/j.scitotenv.2021.144987, 2021.

Ruiz-Reina, A. and López-Ruiz, A.: Short-term river mouth bar development during extreme river discharge events: The role of the phase difference between the peak discharge and the tidal level, Coastal Engineering, 170, 103982, https://doi.org/10.1016/j.coastaleng.2021.103982, 2021.